TITLE: Determination of structural and electronic properties of [Ni(NQSC)2] and [Ni(NQTS)2] complexes with DFT method

AUTHORS: Koray SAYIN,Duran KARAKAS

PAGES: 47-53

**ISSN: 1304-7981** Number: **2**, Year: **2013**, Pages: **47-53** **http://jnrs.gop.edu.tr**

Gaziosmanpasa University
Graduate School of Natural and Applied Sciences
Journal of New Results in Science

*Received*: 05.03.2013
*Accepted*: 20.08.2013

*Editors-in-Chief*: Naim Çağman
*Area Editor*: Yakup Budak

# Determination of structural and electronic properties of $[Ni(NQSC)_2]$ and $[Ni(NQTS)_2]$ complexes with DFT method

**Koray SAYIN**[a,1] (ksayin@cumhuriyet.edu.tr)
**Duran KARAKAŞ**[a] (dkarakas@cumhuriyet.edu.tr)

[a]*Cumhuriyet University, Faculty of Science, Department of Chemistry, 58140 Sivas-TURKEY*

**Abstract** – Nickel (II) complexes of ortho-naphthaquinone semicarbazone and thiosemicarbazone were studied theoretically. $[Ni(NQSC)_2]$ (1) and $[Ni(NQTS)_2]$ (2) complexes were synthesized and geometric parameters, vibrational frequencies and UV-VIS spectrum of mentioned complexes were obtained by Afrasiabi et al. in 2005 [1]. In this study, geometric parameters, vibrational spectrum, Transition Character (TC) analysis and UV-VIS spectrum were calculated as theoretically.

***Keywords*** – *DFT and TD-DFT method, Nickel (II), naphthaquinone semicarbazone and thiosemicarbazone complexes*

## 1. Introduction

Thiosemicarbazones plays important role against bacterial and viral infections [2, 3], tuberculosis [4] and leprosy [5]. The transition metal complexes of thiosemicarbazones indicate greater biological activity than the uncomplexed ligands [1, 6, 7]. Semicarbazone and thiosemicarbazone are similar group. The difference of these molecules is oxygen and sulphur atoms. The biological activity of thiosemicarbazone was studied more than semicarbazone. Semicarbazone of aromatic and unsaturated carbonyl compounds have anticonvulsants properties and their great advantage over the thiosemicarbazone [8, 9]. Structures of semicarbazone and thiosemicarbazone were presented in Figure 1.

---

[1] ***Corresponding Author***

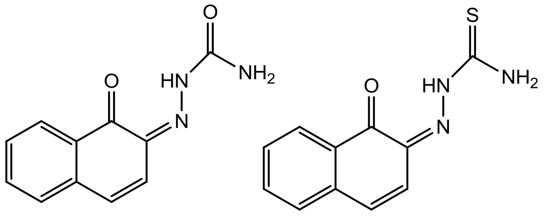

semicarbazone thiosemicarbazone

**Figure 1.** Molecular structures of semicarbazone and thiosemicarbazone.

In report of Afrasiabi et al., vibrational frequencies were assigned and the wavelength of some bands in UV spectrum was given. In this study, the optimized molecular structure of mentioned complexes was obtained with DFT method. The more appropriate basis set was selected by using experimental and theoretically bond lengths and angles. Vibrational spectrum and UV spectrum were calculated by using more appropriate basis set. Theoretical and experimental results were subjected to correlation analysis.

## 2. Computational Details

The input files of mentioned complexes were prepared with GaussView 5.0.8 [10]. All calculations were made by using Gaussian 09 IA32W-G09 RevA. [11]. The complexes performed using Density Functional Theory (DFT) [12] with LANL2DZ [13 – 15] and GEN basis sets. For optimizing with GEN keyword, 6-31g** basis set was selected for S, O, N, C, H atoms and LANL2DZ basis set was selected for Ni atom. All calculations were completed in gas phase. The vibrational frequency analyses indicate that optimized structures of complexes are at stationary points corresponding to local minima without imaginary frequencies. Time Dependent – Density Functional Theory (TD-DFT) [16] method were selected to UV-VIS calculation. UV-VIS spectrum was calculated in dimethylsulfoxide (DMSO). For solution phase, CPCM, which is model corresponds to Polarized Continum Model (PCM), was selected for calculation.

## 3. Result and Discussion

### 3.1. Optimized Structure

Optimized structures were obtained with B3LYP/LANL2DZ and B3LYP/GEN levels. Experimental and theoretical results of bond lengths and angles were compared with each other. For bond lengths and angles, the correlation coefficients (CC) were determined for each level. The CCs were listed in Table 1.

**Table 1**. The correlation coefficients of bond lengths and angles.

| | Basis Set | Bond Length | Bond Angle |
|---|---|---|---|
| [Ni(NQSC)$_2$] | B3LYP/LANL2DZ | 0.8930 | 0.9835 |
| | B3LYP/GEN | 0.8925 | 0.9594 |
| [Ni(NQTS)$_2$] | B3LYP/LANL2DZ | 0.9229 | 0.9850 |
| | B3LYP/GEN | 0.9206 | 0.9848 |

The correlation coefficient of bond lengths and angles indicated that B3LYP/LANL2DZ level is the best level for mentioned complexes. Optimized molecular structure of mentioned complexes was represented in Figure 2 with atomic numbering scheme. The calculated bond lengths and angles of complex 1 in B3LYP/LANL2DZ level were listed in Table 2.

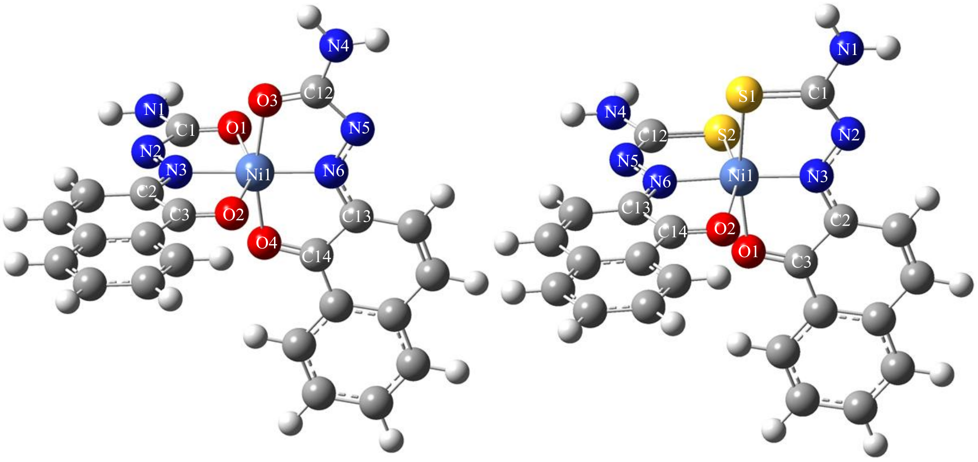

Complex 1

Complex 2

**Figure 2.** Molecular structures of Complex 1 and 2 obtained at B3LYP/LANL2DZ level with atomic numbering scheme.

As can be seen from Table 2, the biggest difference between the experimental and theoretical values occurs at bond length of Ni1 – O3. For this bond the predicted value is longer than the experimental value. Their difference is 0.37 Å for B3LYP/LANL2DZ in gas phase. Mainly the theoretical bond lengths are longer than those of experimental values. As for the bond angles, the biggest difference between experimental and theoretical values mainly takes place at O2 – Ni1 – O1 bond angle. The predicted value is wider than the experimental value. Their difference is 10.6˚ for B3LYP/LANL2DZ level. The calculated bond lengths and angles of complex 2 in B3LYP/LANL2DZ level were listed in Table 3.

**Table 2.** The selected bond lengths and angles at B3LYP/LANL2DZ level.

| Bond Lengths | | | Bond Angles | | |
|---|---|---|---|---|---|
| Assignment | Calc. | Exp. [1] | Assignment | Calc. | Exp. [1] |
| Ni1 – N3 | 1.866 | 1.988 | N3 – Ni1 – N6 | 179.61 | 178.50 |
| Ni1 – N6 | 1.936 | 1.999 | N3 – Ni1 – O3 | 103.91 | 101.90 |
| Ni1 – O3 | 2.437 | 2.067 | N6 – Ni1 – O3 | 75.90 | 76.74 |
| Ni1 – O2 | 1.951 | 2.096 | N3 – Ni1 – O2 | 84.48 | 80.02 |
| Ni1 – O4 | 2.384 | 2.112 | N6 – Ni1 – O2 | 95.86 | 99.40 |
| Ni1 – O1 | 1.972 | 2.137 | O3 – Ni1 – O2 | 91.33 | 92.61 |
| N1 – C1 | 1.356 | 1.320 | N3 – Ni1 – O4 | 101.48 | 102.12 |
| C1 – O1 | 1.295 | 1.241 | N6 – Ni1 – O4 | 78.69 | 79.26 |
| C1 – N2 | 1.409 | 1.415 | O3 – Ni1 – O4 | 154.54 | 155.93 |
| N2 – N3 | 1.333 | 1.278 | O2 – Ni1 – O4 | 92.81 | 93.05 |
| N3 – C2 | 1.353 | 1.335 | N3 – Ni1 – O1 | 81.49 | 75.58 |
| C3 – O2 | 1.308 | 1.260 | N6 – Ni1 – O1 | 98.16 | 104.90 |
| N4 – C12 | 1.374 | 1.336 | O3 – Ni1 – O1 | 90.86 | 88.81 |
| C12 – O3 | 1.267 | 1.238 | O2 – Ni1 – O1 | 165.92 | 155.32 |
| C12 – N5 | 1.420 | 1.402 | O4 – Ni1 – O1 | 91.17 | 95.63 |
| N5 – N6 | 1.327 | 1.293 | - | - | - |
| N6 – C13 | 1.361 | 1.332 | - | - | - |
| C14 – O4 | 1.283 | 1.264 | - | - | - |

**Table 3.** The selected bond lengths and angles at B3LYP/GEN level.

| Bond Lengths | | | Bond Angles | | |
|---|---|---|---|---|---|
| Assignment | Calc. | Exp. [1] | Assignment | Calc. | Exp. [1] |
| Ni1 – N6 | 1.877 | 2.005 | N6 – Ni1 – S2 | 85.72 | 81.09 |
| Ni1 – N3 | 1.927 | 2.021 | N3 – Ni1 – S2 | 94.73 | 101.49 |
| Ni1 – O2 | 1.973 | 2.114 | O2 – Ni1 – S2 | 166.68 | 160.53 |
| Ni1 – O1 | 2.516 | 2.121 | N6 – Ni1 – N3 | 175.01 | 174.80 |
| Ni1 – S1 | 2.588 | 2.377 | N6 – Ni1 – O2 | 84.35 | 79.47 |
| Ni1 – S2 | 2.333 | 2.389 | N3 – Ni1 – O2 | 94.41 | 97.80 |
| S1 – C1 | 1.762 | 1.658 | N6 – Ni1 – O1 | 98.15 | 96.63 |
| S2 – C12 | 1.780 | 1.678 | N3 – Ni1 – O1 | 76.89 | 78.89 |
| O1 – C3 | 1.270 | 1.251 | O2 – Ni1 – O1 | 82.54 | 89.19 |
| O2 – C14 | 1.303 | 1.273 | N6 – Ni1 – S1 | 10.01 | 102.80 |
| N1 – C1 | 1.369 | 1.341 | N3 – Ni1 – S1 | 84.87 | 81.47 |
| N2 – N3 | 1.349 | 1.319 | O2 – Ni1 – S1 | 92.23 | 89.64 |
| N2 – C1 | 1.369 | 1.376 | O1 – Ni1 – S1 | 160.85 | 159.97 |
| N3 – C2 | 1.353 | 1.322 | O1 – Ni1 – S2 | 90.12 | 91.99 |
| N4 – C12 | 1.362 | 1.366 | S1 – Ni1 – S2 | 97.21 | 95.71 |
| N5 – N6 | 1.349 | 1.305 | - | - | - |
| N5 – C12 | 1.363 | 1.345 | - | - | - |
| N6 – C13 | 1.359 | 1.338 | - | - | - |

The biggest difference between the experimental and theoretical values occurs at bond length of Ni1 – O1. For this bond the predicted value is longer than the experimental value. Their difference is 0.395 Å for B3LYP/LANL2DZ. Mainly the theoretical bond lengths are longer than those of experimental values. For the bond angles, the biggest difference between experimental and theoretical values mainly takes place at N3 – Ni1 – S2 bond angle. The predicted value is narrow than the experimental value. Their difference is 6.76° for B3LYP/LANL2DZ level.

### 3.2. IR Studies

The vibrational frequencies were calculated at B3LYP/LANL2DZ level and scaled with 0.9611 [17 – 21]. The calculated frequencies were assigned and represented in Table 3.

**Table 3.** The selected vibrational frequencies (cm$^{-1}$) of mentioned complexes.

| Assignment | Theo. | Exp. [1] | Assignment | Theo. | Exp. [1] |
|---|---|---|---|---|---|
| [Ni(NQSC)$_2$] | | | [Ni(NQTS)$_2$] | | |
| $\nu_{(N-H)}$ | 3486 | 3270 | $\nu_{(N-H)}$ | 3471 | 3393 |
| $\nu_{(N-H)}$ | 3484 | 3325 | $\nu_{(N-H)}$ | 3464 | 3282 |
| $\nu_{(C=O)}$ | 1595 | 1694 | $\nu_{(C=O)}$ | 1514 | 1625 |
| $\nu_{(C=O)}$ | 1590 | 1640 | $\nu_{(C=N)}$ | 1442 | 1580 |
| $\nu_{(C=N)}$ | 1512 | 1600 | $\nu_{(C=S)}$ | 1252 | 1195 |
| $\nu_{(Ni=O)}$ | 650 | 594 | $\nu_{(Ni=O)}$ | 503 | 482 |
| $\nu_{(Ni=O)}$ | 639 | 559 | $\nu_{(Ni=N)}$ | 475 | 436 |
| $\nu_{(Ni=N)}$ | 469 | 451 | $\nu_{(Ni=S)}$ | 322 | 323 |

CC was calculated for complex 1 and 2 and these values are 0.9932 and 0.9946, respectively. According to results, there is a good agreement between experimental and theoretical vibrational frequencies.

### 3.2. UV-VIS Studies

Molecular orbital comprises from the linear combinations of atomic orbital. Different atomic orbital contribute to each MO. Electronic absorption spectrums were calculated by using TD-DFT method with LANL2DZ in DMSO solution. There are two bands in UV-VIS spectrum for complex 1 and 2. The wavelength of bands are 494 and 389 nm for complex 1, 660 and 548 nm for complex 2. The wavelengths of main band are 494 and 548 nm for complex 1 and 2, respectively. Transition character analyses were calculated with Eq. (1) for main bands.

$$\%\text{Transition} = \frac{t^2}{\Sigma t^2} \text{x}100 \qquad (1)$$

Where t is coefficient of the wavefunction for each excitation and $\Sigma t^2$ is the sum of the squares of all coefficient of the wavefunction for each excitation in a specific band. The results show that the maximum transition character has been seen from state 120 to 122 for complex 1 and from state 117 to 120 for complex 2. The contour diagrams of these molecular orbitals were represented in Figure 3.

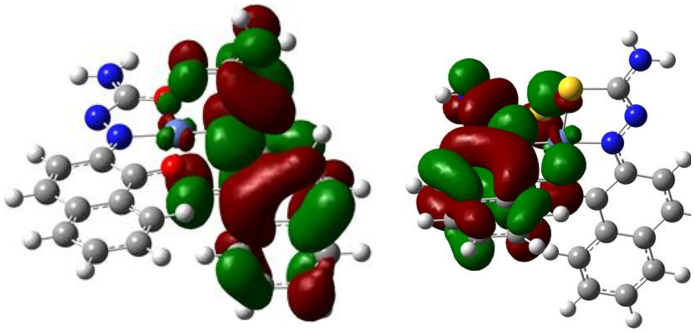

122 (Complex 1) - LUMO+1 120 (Complex 2) - LUMO+1

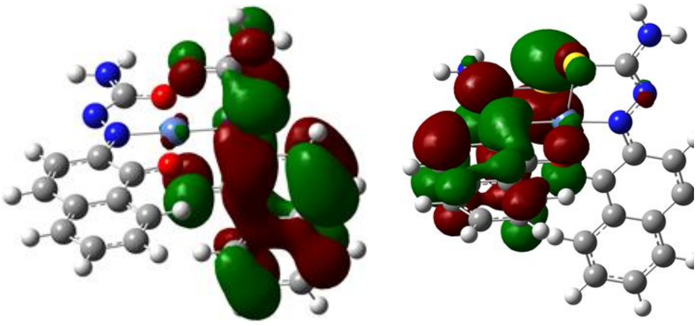

120 (Complex 1) - HOMO 117 (Complex 2) - HOMO-1

**Figure 3.** The contour diagrams of 120, 122 MOs for complex 1 and 117, 120 MOs for complex 2.

According the Figure 3, these transitions are intraligand transitions. In these transitions, π electrons in ligands play an important role.

## 4. Conclusions

DFT and TD-DFT calculations were performed on the relevant complexes, which is [Ni(NQSC)$_2$] and [Ni(NQTS)$_2$] by using B3LYP method with LANL2DZ and GEN basis sets. For structure checking, the calculated structural parameters were used to compare with the experimental structure. Theoretical results are in a good agreement with experimental results at B3LYP/LANL2DZ level. The correlation coefficients of vibrational frequencies were calculated as 0.9932 and 0.9946 for complex 1 and 2, respectively. Electronic absorption spectrum calculations were calculated with TD-DFT method in DMSO solution. The electronic transition characters were analyzed at B3LYP/LANL2DZ level. Two bands were obtained in theoretical electronic absorption spectra for complex 1 and 2. The electronic transition characters and contour diagrams of selected molecular orbitals show that main bands arise from intraligand transitions.

## 5. Acknowledgments

We thank commission of scientific research projects of Cumhuriyet University (Project No: F-308) for financial supports.

## References

**[1]** Z. Afrasiabi, E. Sinn, W. Lin, Y. Ma, C. Campana, S. Padhye, Journal of Inorganic Biochemistry 99 (2005) 1526 – 1531.
**[2]** R. Boon, Antiviral Chem. Chemother., 8 (1997) 5 – 10.
**[3]** C. Shipman, S. H. Smith, J. C. Drach, D. L. Klayman, Antiviral Res., 6 (1986) 197 – 222.
**[4]** A. S. Dobek, D. L. Klayman, E. T. Dickson, J. P. Scovill, C. N. Oster, Arzneim-Forsch 33 (1983) 1583 – 1591.
**[5]** D. L. Klayman, J. P. Scovill, J. F. Bartosevich, C. J. Mason, J. Med. Chem., 22 (1979) 1367 – 73.
**[6]** S. N. Pandeya, J. R. Dimmock, Pharmazie 48 (1993) 659 – 666.
**[7]** A. G. Quiroga, C. N. Ranninger, Coordinat. Chem. Rev., 248 (2004) 119 – 133.
**[8]** J. R. Dimmock, S. C. Vashishta, J. P. Stables, Eur. J. Med. Chem., 35 (2000) 241 – 249.
**[9]** S. K. Sridhar, S. N. Pandeya, J. P. Stables, A. Ramesh, Eur. J. Med. Chem. 16 (2002) 129 – 132.
**[10]** R. D. Dennington II, T.A. Keith, J.M. Millam, GaussView 5.0, Wallingford CT, (2009).
**[11]** M. J. Frisch, G. W. Trucks, H. B. Schlegel, etc., Gaussian, Inc., Wallingford CT, (2009).
**[12]** W. Kohn and L.J. Sham, Phys. Rev. A 137 (1965) 1697 – 1705.
**[13]** A. D. Becke, J. Chem. Phys. 98 (1993) 5648 – 5652.
**[14]** C. Lee, W. Yang and R. G. Parr, Phys. Rev. B, 37 (1988) 785 – 789.
**[15]** P. J. Hay and W. R. Wadt, J. Chem. Phys., 82 (1985) 270 – 283.
**[16]** D. Jacquemin, V. Wathelet, E. A. Perpète and C. Adamo, J. Chem. Theory Comput., 5 (2009) 2420 – 2435.
**[17]** M. D. Halls, J. Velkovski, H. B. Schlegel, Theor. Chem. Acc., 105 (2001) 413 – 421.
**[18]** P. Sinha, S. E. Boesch, C. M. Gu, R. A. Wheeler, A. K. Wilson, J. Phys. Chem. A, 108 (2004) 9213 – 9217.
**[19]** M. P. Andersson, P. Uvdal, J. Phys. Chem. A, 109 (2005) 2937 – 2941.
**[20]** Y. N. Panchenko, V. I. Pupyshev, C. W. Bock, J. Mol. Struct., 550 (2000) 495 – 504.
**[21]** K. V. Berezin, V. V. Nechaev, T. V. Krivokhizhina, Opt. Spectrosc., 94 (2003) 357 – 360.